

## Geodesic Evolution Laws—A Level-Set Approach\*

Christina Stöcker<sup>†</sup> and Axel Voigt<sup>‡</sup>

**Abstract.** Motion of curves governed by geometric evolution laws, such as mean curvature flow and surface diffusion, is the basis for many algorithms in image processing. If the images to be processed are defined on nonplanar surfaces, the geometric evolution laws have to be restricted to the surface and turn into geodesic evolution laws. In this paper we describe efficient algorithms for geodesic mean curvature flow and geodesic surface diffusion within a level-set approach. Thereby we compare approaches with an explicit representation of the surface by a triangulated surface mesh and an implicit surface representation as the zero-level surface of a level-set function. As an application we present the numerical treatment of the classical model of Rudin, Osher, and Fatemi to denoise images on surfaces.

**Key words.** image denoising, PDEs on surfaces, higher order equations, geodesic evolution laws, level-set method, finite elements, adaptivity

**AMS subject classifications.** 35K55, 53C44, 53D25

**DOI.** 10.1137/070699640

**1. Introduction.** Planar motion of curves is the basis for many image processing algorithms. Examples include algorithms for image denoising, image restoration, and image decomposition; see, e.g., [23, 29] and [35, 20, 30, 6] and the references therein for a review. The underlying geometric evolution laws in many of these models are typically of second order and are versions of mean curvature flow. Various numerical approaches have been developed for these equations and today are widely used in image processing for planar images. If images defined on nonplanar surfaces have to be processed, the developed evolution laws for planar images can easily be modified by replacing the operators by their geometric counterparts, e.g., the Laplacian by the surface Laplacian. Instead of planar motion of curves we now have to deal with the evolution of curves which are restricted to surfaces. The problem of mean curvature flow, for example, becomes a geodesic mean curvature flow problem. Analytical results and computational algorithms for the equations on surfaces require more care, which is due to the additional nonlinearity of the surface operators.

Different approaches have been developed to deal with the motion of curves in image processing on nonplanar surfaces. One requires the representation of the surface by a surface mesh. For example, [10, 13, 27, 15] use this approach to solve (an)isotropic geometric diffusion

---

\*Received by the editors August 8, 2007; accepted for publication (in revised form) August 20, 2008; published electronically December 19, 2008. This work was supported by the EU through “STRP 016447” and DFG through “VO899/6-1” and “VO899/5-1.”

<http://www.siam.org/journals/siims/1-4/69964.html>

<sup>†</sup>Crystal Growth group, Research Center caesar, Ludwig-Erhard-Allee 2, 53175 Bonn, Germany. Current address: Institut für Numerische und Angewandte Mathematik, Universität Münster, 48147 Münster, Germany ([christina.stoecker@uni-muenster.de](mailto:christina.stoecker@uni-muenster.de)).

<sup>‡</sup>Institut für Wissenschaftliches Rechnen, Technische Universität Dresden, Zellescher Weg 12-14, 01062 Dresden, Germany ([Axel.Voigt@tu-dresden.de](mailto:Axel.Voigt@tu-dresden.de)).

problems on surfaces, which is related to the motion of curves on surfaces. Reference [16] uses this approach to solve geodesic mean curvature flow. In an alternative approach, a mapping between a parameterization plane and the surface can be used; see, e.g., [8, 19] for related second order image processing problems on surfaces. Reference [32] uses this approach to solve geodesic mean curvature flow and related problems. Another widely used approach in image processing is the level-set method introduced in [25]. This is partly due to the simplicity of implementing it by finite differences on Cartesian grids. This simplicity, however, is lost if images defined on nonplanar surfaces have to be processed. However, one can represent the surface as well as the data on it implicitly as level sets of functions in  $\mathbb{R}^3$  and reformulate the equation on a surface into an equation in  $\mathbb{R}^3$ ; see [4]. In [7] this approach is used to solve the problem of geodesic mean curvature flow. Similar ideas for representing the surface only implicitly through a level-set function have also been used in phase-field methods [27]. To summarize for second order problems, a large class of methods exists which can be used in image processing algorithms to evolve curves on nonplanar surfaces. A detailed comparison of the methods and convergence studies are, however, still missing. Most of the approaches described can also be combined with an evolution of the surface, e.g., to smooth the surface. See, e.g., [2, 16] for an approach in which the surface mesh is moved and [1, 36, 33, 28] for an implicit surface representation. In the last examples the evolution of the surface depends on the quantities on it.

More recent image processing models designed for image restoration and image decomposition contain not only the mean curvature but also the Laplacian of mean curvature which results in fourth order equations [26]. The authors of [26] also apply the model to image denoising and show that for textured images it gives better results than the classical second order models. Furthermore, an application of fourth order PDEs to medical imaging and inpainting can be found in [22, 5], respectively. In order to extend the use of these models to images on surfaces, numerical methods for geodesic generalizations are required. The problem of surface diffusion (Laplacian of mean curvature) now becomes geodesic surface diffusion (surface Laplacian of geodesic mean curvature). Numerical approaches for fourth order problems on surfaces, especially geodesic surface diffusion problems, are very limited. Based on the ideas of [14], parametric finite elements can be used to solve general PDEs on triangulated surfaces; see [16] for such an approach for solving geodesic mean curvature flow and also geodesic surface diffusion and [34] for implementation details for solving general problems on surface meshes by finite elements. We are not aware of a treatment of fourth order equations on surfaces using a mapping between a parameterization plane and the surface. In the case of implicit surface representations through level-set or phase-field functions, we refer to [18, 27, 17], where a Cahn–Hilliard equation on a surface is solved. The approach is extended in [21] to solve a Cahn–Hilliard equation on a moving surface, with the surface evolution coupled to the concentration field on the surface. The treatment of geodesic surface diffusion has not been considered within the concept of an implicit surface representation.

In this article we will consider only stationary surfaces and compare level-set solutions for geodesic mean curvature flow and geodesic surface diffusion obtained by an explicit and an implicit representation of the surface. For both approaches we use finite elements to discretize the evolution law in space. Thereby the advantages of finite elements implemented in the advanced simulation toolbox AMDiS [34] are demonstrated. Here the solution of any PDE

on a triangulated surface can be done with the same code as its solution on a planar domain. The work can be seen as a general approach to implementing image processing algorithms on surfaces. As an example we apply the classical Rudin–Osher–Fatemi (ROF) model [29], which can be considered as mean curvature flow with a forcing term, to denoise images on various surfaces.

The article is organized as follows: In section 2 we review the level-set formulation for mean curvature flow and surface diffusion and show the relation to a level-set formulation for geodesic mean curvature flow and geodesic surface diffusion by replacing the standard operators by their intrinsic counterparts. Furthermore, we use the approach of [4] to translate the formulation for an implicit surface representation. In section 3 we discuss the weak formulation for the two equations and in section 4 we describe the discretization and the solution of the resulting linear system. Section 5 shows numerical results, and, finally, section 6 deals with a finite element treatment of the ROF model on implicit surfaces and gives numerical results for image denoising.

**2. Level-set method.** We start by reviewing standard level-set methods for geometric evolution laws, such as mean curvature flow and surface diffusion. In the next step we extend the concept to geodesic evolution laws on surfaces and on implicitly defined surfaces.

**2.1. Level-set method for geometric evolution laws.** Let us start with the classical problem of defining the motion of a surface. We consider the level-set equation for a level-set function  $\phi$  defined in  $\mathbb{R}^{n+1}$  with  $\phi = 0$  representing the  $n$ -dimensional surface  $\Gamma$ :

$$(2.1) \quad \phi_t + V|\nabla\phi| = 0$$

with a given normal velocity  $V$ . This equation was introduced for numerical surface evolution in [25]. It describes the surface and its evolution by the implicit function  $\phi$ . Through  $\phi$  we can define the normal and the curvature to each level line and thus also to the surface  $\Gamma$  by

$$\nu = \frac{\nabla\phi}{|\nabla\phi|}, \quad \kappa = \nabla \cdot \frac{\nabla\phi}{|\nabla\phi|}.$$

If we now specify  $V$ , we can use the level-set equation to solve the geometric evolution laws of interest. A classical geometric evolution equation is motion by mean curvature. The normal velocity of the surface  $\Gamma$  is given by minus its mean curvature:

$$V = -\kappa.$$

Using the level-set equation (2.1) and the definition for the curvature we obtain the level-set representation for mean curvature flow:

$$\frac{\phi_t}{|\nabla\phi|} = \nabla \cdot \frac{\nabla\phi}{|\nabla\phi|}.$$

Similar calculations can be done for motion by surface diffusion. The normal velocity of the surface  $\Gamma$  is given by the surface Laplacian of  $\Gamma$  applied to the mean curvature:

$$V = \Delta_\Gamma \kappa.$$

In level-set representation this equation reads, rewritten as a system of two second order equations for  $\phi$  and  $\psi$ , as

$$\begin{aligned}\phi_t &= \nabla \cdot (|\nabla\phi|(I - \nu \otimes \nu)\nabla\psi), \\ \psi &= \nabla \cdot \frac{\nabla\phi}{|\nabla\phi|}.\end{aligned}$$

For a review of numerical approaches for mean curvature flow, see [12]. Numerical approaches for surface diffusion have been developed using finite differences in [9, 31] and finite elements in [11]. As the evolution of  $\Gamma$  is implicitly represented as the evolution of the zero-level line of  $\phi$ , the problem to solve is defined on  $\mathbb{R}^{n+1}$  and is thus typically less efficient than directly solving the geometric evolution law on a triangulated surface. However, such a direct approach is not always applicable, e.g., if topology changes occur. The computational overhead of the level-set method furthermore can be reduced by using narrow band approaches or adaptive mesh refinement strategies which make the numerical costs comparable to those of direct methods.

**2.2. Level-set method for geodesic evolution laws.** In the same way as in  $\mathbb{R}^{n+1}$  we can consider a level-set equation for a level-set function  $u$  defined on a surface  $\Gamma$  with  $u = 0$  representing the curve  $C$  on  $\Gamma$  (see, e.g., [3, 16]):

$$(2.2) \quad u_t + V_g |\nabla_\Gamma u| = 0$$

with intrinsic normal velocity  $V_g$ .  $\nabla_\Gamma$  denotes the surface gradient of  $\Gamma$ . Here we assume  $\Gamma$  to be stationary. Through  $u$  we can define the intrinsic normal and the intrinsic curvature (geodesic curvature) to each level line of  $u$  and thus also to the curve  $C$ :

$$\nu_g = \frac{\nabla_\Gamma u}{|\nabla_\Gamma u|}, \quad \kappa_g = \nabla_\Gamma \cdot \frac{\nabla_\Gamma u}{|\nabla_\Gamma u|}.$$

As for surfaces in  $\mathbb{R}^{n+1}$ , we can define geometric evolution laws (so-called geodesic evolution laws) for the curve  $C$ , now restricted to  $\Gamma$ . Geodesic mean curvature flow thus reads as

$$V_g = -\kappa_g,$$

which relates the intrinsic normal velocity to minus the geodesic curvature. Using the level-set equation on the surface (2.2), we thus obtain the level-set representation for geodesic mean curvature flow

$$\frac{u_t}{|\nabla_\Gamma u|} = \nabla_\Gamma \cdot \frac{\nabla_\Gamma u}{|\nabla_\Gamma u|}.$$

In a similar way we can consider motion by geodesic surface diffusion

$$V_g = \Delta_g \kappa_g.$$

Here the intrinsic normal velocity is given by the intrinsic Laplacian of  $C$  on  $\Gamma$  of the geodesic curvature. Thus  $\Delta_g$  depends on  $C$  and  $\Gamma$ . In level-set representation, geodesic surface diffusion

reads, rewritten as a system of two second order equations for  $u$  and  $v$ , as

$$\begin{aligned} u_t &= \nabla_\Gamma \cdot (|\nabla_\Gamma u|(I - \nu_g \otimes \nu_g)\nabla_\Gamma v), \\ v &= \nabla_\Gamma \cdot \frac{\nabla_\Gamma u}{|\nabla_\Gamma u|}. \end{aligned}$$

A finite element discretization for these equations is derived in [16]. It should be noted that any modern finite element implementation of the level-set equation in  $\mathbb{R}^{n+1}$  on unstructured meshes can also solve the level-set equation on triangulated surfaces. For implementational details see [34]. The only requirement is an appropriate surface mesh. Figures 5, 6, 7, and 8 show results of geodesic mean curvature flow and geodesic surface diffusion, computed with the algorithm initially developed in AMDiS [34] for mean curvature flow and surface diffusion [11].

In this approach the evolution of a curve  $C$  on a surface  $\Gamma$  is implicitly represented as the evolution of the zero-level line of  $u$ , with  $u$  defined on  $\Gamma$ . Thus the methods require a surface triangulation, which might not be available or easy to generate for complex geometries. We thus now want to reduce this requirement and define the surface  $\Gamma$  only implicitly following the approach in [4].

**2.3. Level-set method for geodesic evolution laws on implicit surfaces.** Let the surface  $\Gamma$  be defined as the zero-level line of the level-set function  $\phi$  defined in  $\mathbb{R}^{n+1}$ . With  $u$  the level-set function extended also to  $\mathbb{R}^{n+1}$ , the curve  $C$  thus is defined as  $C = \{x \in \mathbb{R}^{n+1} : \phi(x) = u(x) = 0\}$ . The level-set equation (2.2) now reads in its extended version to  $\mathbb{R}^{n+1}$  as

$$(2.3) \quad u_t + V_g|(I - \nu \otimes \nu)\nabla u| = 0.$$

Through  $u$  and  $\phi$  we can define the intrinsic normal and the intrinsic curvature (geodesic curvature) to each level line of  $u$  and  $\phi$  and thus also to the curve  $C$ :

$$\nu_g = \frac{(I - \nu \otimes \nu)\nabla u}{|(I - \nu \otimes \nu)\nabla u|}, \quad \kappa_g = \frac{1}{|\nabla\phi|} \nabla \cdot \left( |\nabla\phi| \frac{(I - \nu \otimes \nu)\nabla u}{|(I - \nu \otimes \nu)\nabla u|} \right).$$

The level-set representation for geodesic mean curvature flow on an implicitly defined surface thus reads as

$$(2.4) \quad \frac{u_t}{|(I - \nu \otimes \nu)\nabla u|} = \frac{1}{|\nabla\phi|} \nabla \cdot \left( |\nabla\phi| \frac{(I - \nu \otimes \nu)\nabla u}{|(I - \nu \otimes \nu)\nabla u|} \right),$$

which has already been derived in [7]. In the same way we obtain the level-set representation for geodesic surface diffusion on implicitly defined surfaces as

$$(2.5) \quad u_t = \frac{1}{|\nabla\phi|} \nabla \cdot (|\nabla\phi| |(I - \nu \otimes \nu)\nabla u|(I - \nu_g \otimes \nu_g)(I - \nu \otimes \nu)\nabla v),$$

$$(2.6) \quad v = \frac{1}{|\nabla\phi|} \nabla \cdot \left( |\nabla\phi| \frac{(I - \nu \otimes \nu)\nabla u}{|(I - \nu \otimes \nu)\nabla u|} \right).$$

We have reduced the problem of evolving a curve along a surface to a problem in  $\mathbb{R}^{n+1}$ . In other words, we have reformulated an initially one-dimensional problem into a three-dimensional problem. The computational overhead thus has to be reduced by efficient numerical tools for the evolution equation, such as narrow band or adaptive mesh refinement

strategies. Through the reformulation we gain the flexibility to handle complex surfaces, circumventing the need to construct an appropriate surface mesh.

The problem of geodesic mean curvature flow was already introduced and solved within a finite difference method in [7]. The problem of geodesic surface diffusion, however, has not been solved yet.

### 3. Weak formulation.

**3.1. Mean curvature flow and surface diffusion.** Only to show the analogy between the formulation in  $\mathbb{R}^{n+1}$  and on surfaces, we recall first the weak forms for mean curvature flow and surface diffusion used in [11]:

$$\int_{\Omega} \frac{\phi_t \eta}{|\nabla \phi|} dx = - \int_{\Omega} \frac{\nabla \phi \cdot \nabla \eta}{|\nabla \phi|} dx$$

and

$$\begin{aligned} \int_{\Omega} \phi_t \eta dx &= - \int_{\Omega} |\nabla \phi| (I - \nu \otimes \nu) \nabla \psi \cdot \nabla \eta dx, \\ \int_{\Omega} \psi \xi dx &= \int_{\Omega} \frac{\nabla \phi \cdot \nabla \xi}{|\nabla \phi|} dx, \end{aligned}$$

respectively, with test functions  $\eta$  and  $\xi$  defined in the domain of interest  $\Omega \subseteq \mathbb{R}^{n+1}$ .

**3.2. Level-set method for geodesic evolution laws on explicit surfaces.** The weak forms for geodesic mean curvature flow and geodesic surface diffusion on explicit surfaces thus follow by replacing the operators by their geometric counterparts and read as

$$\int_{\Gamma} \frac{u_t \eta}{|\nabla_{\Gamma} u|} dA = - \int_{\Gamma} \frac{\nabla_{\Gamma} u \cdot \nabla_{\Gamma} \eta}{|\nabla_{\Gamma} u|} dA$$

and

$$\begin{aligned} \int_{\Gamma} u_t \eta dA &= - \int_{\Gamma} |\nabla_{\Gamma} u| (I - \nu \otimes \nu) \nabla_{\Gamma} \psi \cdot \nabla_{\Gamma} \eta dA, \\ \int_{\Gamma} \psi \xi dA &= \int_{\Gamma} \frac{\nabla_{\Gamma} u \cdot \nabla_{\Gamma} \xi}{|\nabla_{\Gamma} u|} dA, \end{aligned}$$

respectively, with test functions  $\eta$  and  $\xi$  defined on the surface  $\Gamma$ . The same forms have been used in [16].

**3.3. Level-set method for geodesic evolution laws on implicit surfaces.** The implicitly defined surface is embedded into a simple domain  $\Omega$ . The weak forms of (2.4) and (2.5)–(2.6), which here are equations in  $\Omega$ , read as

$$\int_{\Omega} \frac{u_t |\nabla \phi|}{|(I - \nu \otimes \nu) \nabla u|} \eta dx = - \int_{\Omega} |\nabla \phi| \frac{(I - \nu \otimes \nu) \nabla u}{|(I - \nu \otimes \nu) \nabla u|} \cdot \nabla \eta dx$$

and

$$\begin{aligned} \int_{\Omega} |\nabla\phi| u_t \eta \, dx &= \int_{\Omega} |\nabla\phi| (I - \nu \otimes \nu) \nabla u (I - \nu_g \otimes \nu_g) (I - \nu \otimes \nu) \nabla v \cdot \nabla \eta \, dx, \\ \int_{\Omega} |\nabla\phi| v \xi \, dx &= - \int_{\Omega} |\nabla\phi| \frac{(I - \nu \otimes \nu) \nabla u}{|(I - \nu \otimes \nu) \nabla u|} \cdot \nabla \xi \, dx, \end{aligned}$$

respectively, with test functions  $\eta$  and  $\xi$  defined in  $\Omega$ .

**4. Discretization.** We present the discretization for geodesic mean curvature flow and geodesic surface diffusion on implicit surfaces. The domain  $\Omega$  is chosen in a way which allows for easy triangulation. This is no restriction because the only requirement on  $\Omega$  is that it contain the surface  $\Gamma$ . We further use standard linear finite elements and denote  $\mathcal{V}^h$  as the  $N$ -dimensional finite element space on the triangulated domain  $\Omega$ . We apply a semi-implicit time discretization and, as small gradients may occur, regularize the Euclidean norm  $|\cdot|$  through  $|x|_{\epsilon} = (|x|^2 + \epsilon^2)^{1/2}$  with  $\epsilon$  chosen about the grid size  $h$ . The discretized equations for geodesic mean curvature flow are then given through

$$(4.1) \quad \begin{aligned} \int_{\Omega} \frac{u^{k+1} |\nabla\phi|_{\epsilon}}{|(I - \nu \otimes \nu) \nabla u^k|_{\epsilon}} \eta \, dx - \int_{\Omega} \frac{u^k |\nabla\phi|_{\epsilon}}{|(I - \nu \otimes \nu) \nabla u^k|_{\epsilon}} \eta \, dx \\ + \tau \int_{\Omega} |\nabla\phi|_{\epsilon} \frac{(I - \nu \otimes \nu) \nabla u^{k+1}}{|(I - \nu \otimes \nu) \nabla u^k|_{\epsilon}} \cdot \nabla \eta \, dx = 0. \end{aligned}$$

For the description of the arising linear system we introduce the following notation for the mass and stiffness matrices. For a function  $f : \Omega \rightarrow \mathbb{R}$ , a linear operator  $A : \mathbb{R}^3 \rightarrow \mathbb{R}^3$ , and  $(\varphi_i)_{i=1, \dots, N}$  basis functions of  $\mathcal{V}^h$ , we set

$$\begin{aligned} M[f] &:= \left( \int_{\Omega} f \varphi_i \varphi_j \, dx \right)_{ij}, \\ L[A] &:= \left( \int_{\Omega} A \nabla \varphi_i \cdot \nabla \varphi_j \, dx \right)_{ij}. \end{aligned}$$

With the linear expansion  $u = \sum_{i=1}^N \bar{u}_i \varphi_i$  and

$$\begin{aligned} M_1 &:= M[|\nabla\phi|_{\epsilon} |(I - \nu \otimes \nu) \nabla u^k|_{\epsilon}^{-1}], \\ L_1 &:= L[|\nabla\phi|_{\epsilon} |(I - \nu \otimes \nu) \nabla u^k|_{\epsilon}^{-1} (I - \nu \otimes \nu)], \end{aligned}$$

the linear system corresponding to (4.1) then reads as

$$(M_1 + \tau L_1) \bar{u}^{k+1} = M_1 \bar{u}^k.$$

We solve the linear system with the Krylov subspace method BiCGStab2.

In a similar way the discretization for geodesic surface diffusion results in

$$(4.2) \quad \begin{aligned} \int_{\Omega} |\nabla\phi|_{\epsilon} u^{k+1} \eta \, dx - \int_{\Omega} |\nabla\phi|_{\epsilon} u^k \eta \, dx \\ - \tau \int_{\Omega} |\nabla\phi|_{\epsilon} (I - \nu \otimes \nu) \nabla u^k |_{\epsilon} (I - \nu_g^k \otimes \nu_g^k) (I - \nu \otimes \nu) \nabla v^{k+1} \cdot \nabla \eta \, dx = 0, \end{aligned}$$

$$(4.3) \quad \int_{\Omega} |\nabla\phi|_{\epsilon} v^{k+1} \xi \, dx + \int_{\Omega} |\nabla\phi|_{\epsilon} \frac{(I - \nu \otimes \nu) \nabla u^{k+1}}{|(I - \nu \otimes \nu) \nabla u^k|_{\epsilon}} \cdot \nabla \xi \, dx = 0,$$

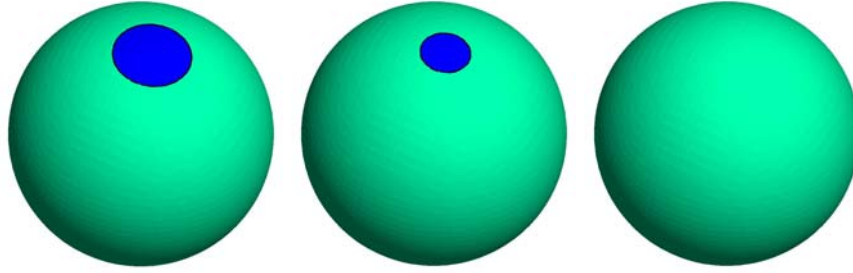


**Figure 1.** Geodesic mean curvature flow with level-set representation of the surface: evolution of circle.  $[0, 4] \times [0, 4] \times [0, 4]$  grid with 30,000 grid points, grid size  $h = 0.0625$  at the surface, and timestep  $\Delta t = h^2 = 0.0039$ . From left to right:  $t = 0.0$ ,  $t = 0.0273$ ,  $t = 0.0468$ .

where  $\nu_g^k = \frac{(I - \nu \otimes \nu) \nabla u^k}{|(I - \nu \otimes \nu) \nabla u^k|}$  is the intrinsic surface normal in the last timestep. With the linear expansions  $u = \sum_{i=1}^N \bar{u}_i \varphi_i$  and  $v = \sum_{i=1}^N \bar{v}_i \varphi_i$  and the matrices

$$\begin{aligned} M_1 &:= M[|\nabla \phi|_\epsilon], \\ L_1 &:= L[|\nabla \phi|_\epsilon (I - \nu \otimes \nu) \nabla u^k|_\epsilon (I - \nu_g^k \otimes \nu_g^k) (I - \nu \otimes \nu)], \\ L_2 &:= L[|\nabla \phi|_\epsilon (I - \nu \otimes \nu) \nabla u^k|_\epsilon (I - \nu \otimes \nu)], \end{aligned}$$

the linear system corresponding to (4.2) and (4.3) reads as

$$\begin{pmatrix} M_1 & -\tau L_1 \\ L_2 & M_1 \end{pmatrix} \begin{pmatrix} \bar{u}^{k+1} \\ \bar{v}^{k+1} \end{pmatrix} = \begin{pmatrix} M_1 \bar{u}^k \\ 0 \end{pmatrix}.$$

The linear system is solved with a Schur complement approach

$$(M_1 + \tau L_1 M_1^{-1} L_2) \bar{u}^{k+1} = M_1 \bar{u}^k$$

and the Krylov subspace method BiCGStab2.

## 5. Numerical results.

**5.1. Geodesic mean curvature flow.** To validate our computations for geodesic mean curvature flow on implicit surfaces, we regard the evolution of a circle on a sphere, where the exact solution can be calculated easily, and compare our computational results for different grid sizes and timesteps with the exact evolution. The evolution of a circle with initial radius  $R_0$  on a sphere with radius  $r$  gives at time  $t$  a circle with radius

$$R(t) = \left( r^2 - \left( \frac{t}{r} \right) + (r^2 - R_0^2)^{1/2} \right)^{1/2}.$$

In our example we choose  $r = 1.0$  and  $R_0 = 0.3$ . The evolution is shown in Figure 1 which displays the solution on the zero-level set. The solution is analyzed in Figure 2 and Table 1. The results show that the choice of grid size  $h = 0.0625$  and timestep  $\Delta t = h^2$  is appropriate.

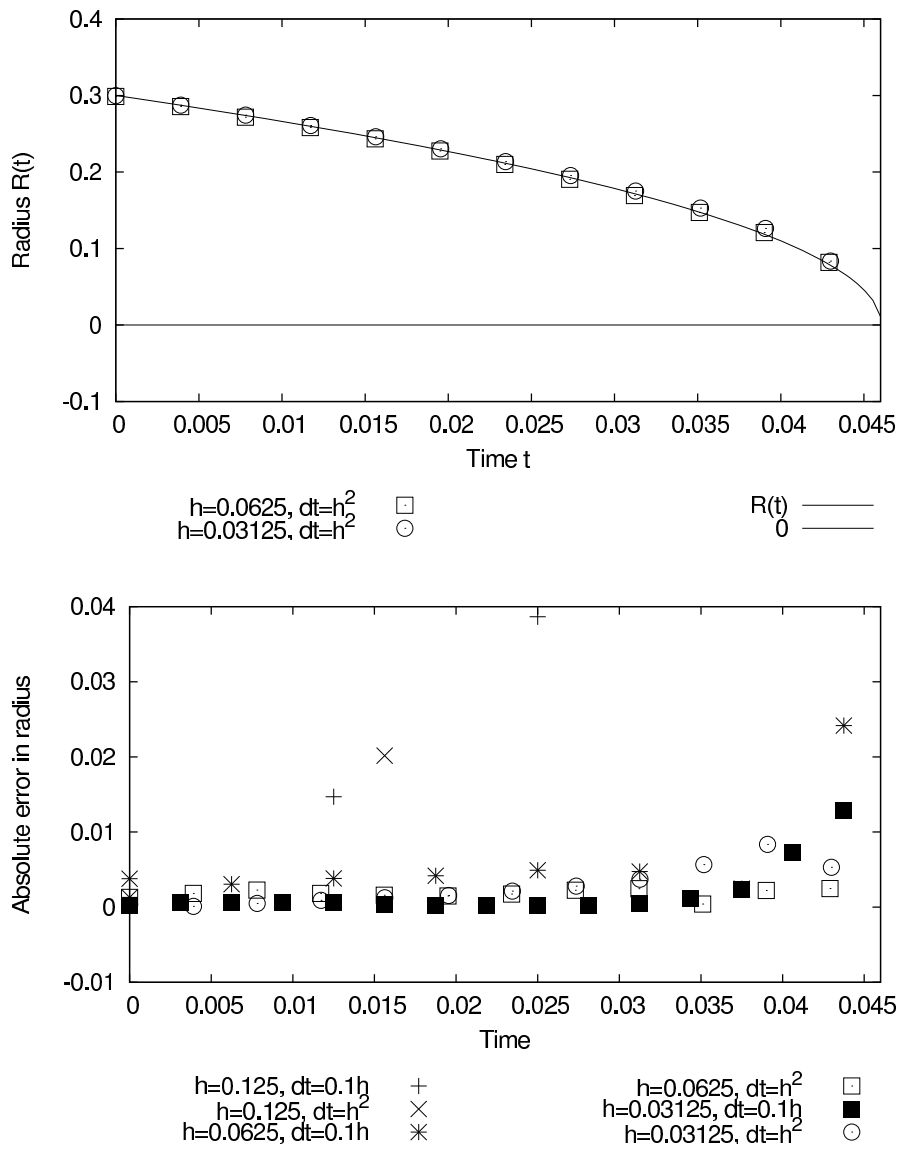


**Figure 2.** Geodesic mean curvature flow with level-set representation of the surface: evolution of a circle with initial radius  $R_0 = 0.3$  on a sphere with radius  $r = 1.0$  with different grid sizes and timesteps; see Figure 1. Above: comparison of the exact evolution of the circle with computational results with grid sizes  $h = 0.0625$  and  $h = 0.03125$  and timestep  $\Delta t = h^2$ . Below: absolute error in the radius with grid sizes  $h = 0.125, 0.0625,$  and  $0.03125$  and timesteps  $\Delta t = 0.1h$  and  $h^2$ , respectively.

**Table 1**

Results at time  $t = 0.0156$  with  $R(t) = 0.24494$  for the problem in Figure 1.

$h$	Computational radius	$err(h)$
0.125	0.22467	0.02026
0.0625	0.24335	0.00159
0.03125	0.24606	0.00113

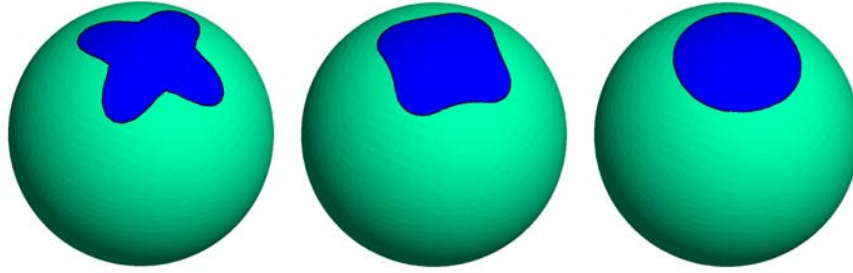


**Figure 3.** Geodesic surface diffusion with level-set representation of the surface: evolution of star-shaped closed curve.  $[0, 4] \times [0, 4] \times [0, 4]$  grid with 30,000 grid points, grid size  $h = 0.0625$  at the surface, and timestep  $\Delta t = h^4 = 1.5 \times 10^{-5}$ . From left to right:  $t = 0.0$ ,  $t = 0.0003$ ,  $t = 0.00105$ .

The error analysis is based on the computationally measured area  $A(t)$  enclosed by the evolving circle on the implicit surface. The radius of the circle at time  $t$  is calculated through

$$R(t) = \left( r^2 - \left( r - \frac{A(t)}{2\pi r} \right)^2 \right)^{1/2}.$$

Thus the error is measured only on the implicit surface and not on the complete mesh.

**5.2. Geodesic surface diffusion.** To validate our computations for geodesic surface diffusion on implicit surfaces, we check the volume conservation property. We regard the example in Figure 3 for different grid sizes and timesteps. The volume-conserving behavior is presented in Figure 4 and Table 2. Again, Figure 4 shows that the choice of grid size  $h = 0.0625$  and timestep  $\Delta t = h^4$  is appropriate.

Here  $err(h)$  denotes the absolute error in the computationally measured area enclosed by the evolving closed curve and grid size  $h$  at the implicit surface. The error is calculated with respect to the initial discrete area enclosed by the curve at time  $t = 0$ , which should be preserved. We should note that the initial discrete area depends on grid size  $h$ .

**5.3. Comparison of geodesic mean curvature flow and geodesic surface diffusion on explicit and implicit surfaces.** As a second test we compare solutions obtained for geodesic mean curvature flow and geodesic surface diffusion on different explicit and implicit surfaces; see Figures 5, 6, 7, and 8. In Figures 7 and 8 the initial closed curves on the torus are circles with a superposition of the sine function with two different frequencies. As expected, first the high frequencies are damped before the lower frequencies vanish on a larger time scale.

**5.4. Adaptivity.** To make the simulations efficient, we use adaptively refined grids. The criterion for refinement is the distance to the level set of interest. This strategy ensures a coarse mesh away from the surface and thus reduces the computational overhead introduced due to the higher dimension. The computational domain thus can be large enough such that the boundary condition has no influence on the solution on the surface of interest and is usually a simple cube. For an example of such a grid, see Figure 9. Compared with a narrow band approach to restrict the computational domain to a thin region around the surface, the

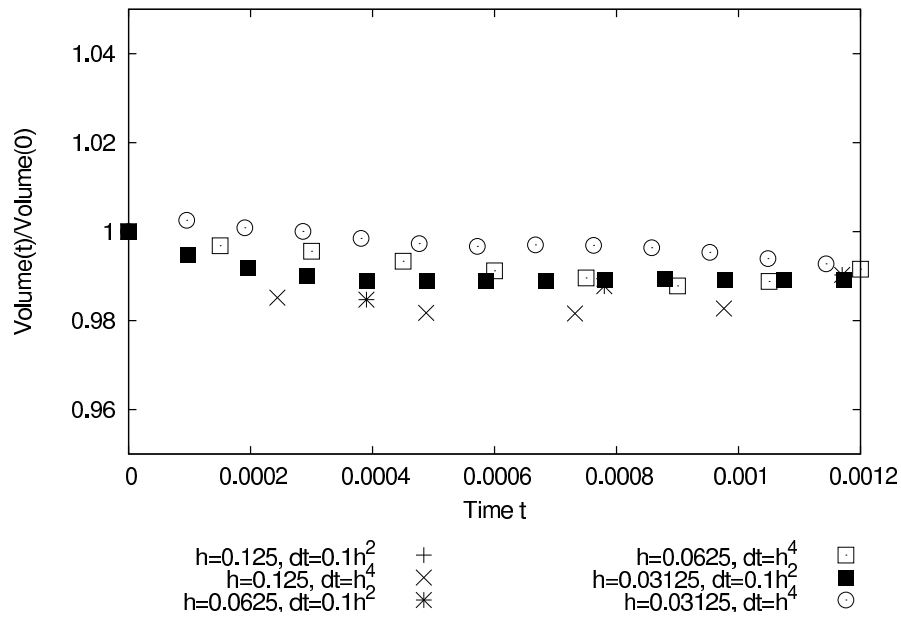


**Figure 4.** Geodesic surface diffusion with level-set representation of the surface: volume conservation for the example in Figure 3 for different grid sizes  $h = 0.125, 0.0625, \text{ and } 0.03125$  and timesteps  $\Delta t = 0.1h^2$  and  $h^4$ , respectively.

**Table 2**

Results at time  $t = 0.00105$ , for the problem in Figure 4.

$h$	Computational initial area	$err(h)$
0.125	0.76284	0.01318
0.0625	0.78831	0.00882
0.03125	0.79730	0.00482

adaptive mesh has the advantage that no further boundary conditions have to be specified on the edge of the computational domain.

Figures 10 and 11 show the evolution of a sine function on the Stanford bunny under geodesic mean curvature flow and geodesic surface diffusion, respectively.

**6. Denoising of surface images.** For the denoising of images Rudin, Osher, and Fatemi proposed a time-dependent model in [29]. With its adaption in [24] to circumvent strong timestep restrictions, it can be regarded as mean curvature flow with a forcing term. For an initial noisy image  $u_0$ , the evolution equation in  $\mathbb{R}^{n+1}$  in level-set formulation is

$$u_t = |\nabla u| \left( \nabla \cdot \frac{\nabla u}{|\nabla u|} - 2\lambda(u - u_0) \right)$$

with the forcing term coefficient  $\lambda$ . The equation can also be applied on surfaces, which gives

$$u_t = |\nabla_{\Gamma} u| \left( \nabla_{\Gamma} \cdot \frac{\nabla_{\Gamma} u}{|\nabla_{\Gamma} u|} - 2\lambda(u - u_0) \right),$$

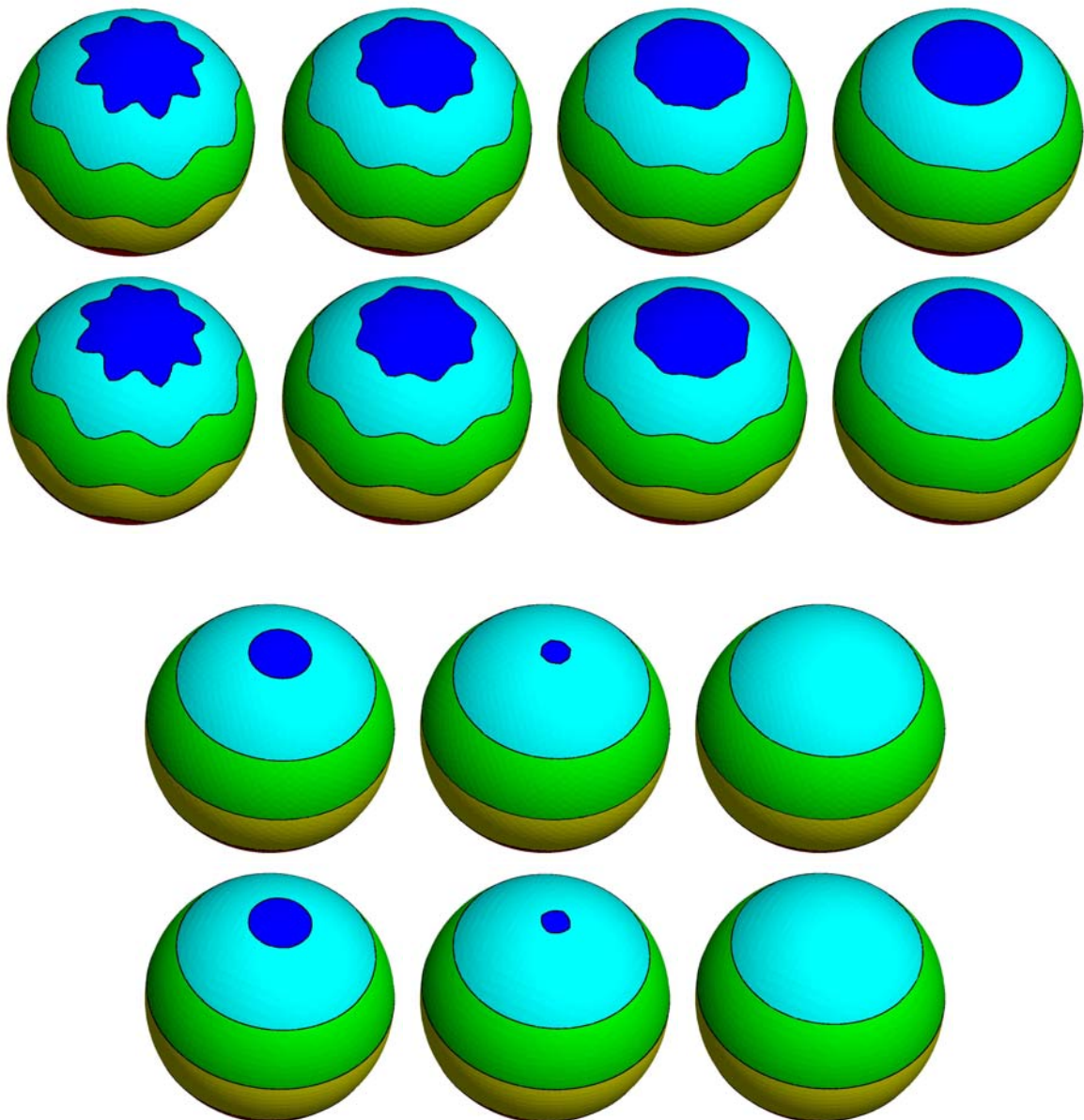


**Figure 5.** Geodesic mean curvature flow with parameterization of the surface (first and third rows) and level-set representation of the surface (second and fourth rows). Parametric approach: 3,000 grid points, grid size  $h = 0.064$ , and timestep  $\Delta t = 0.004$ . Level-set approach:  $[0, 4] \times [0, 4] \times [0, 4]$  grid with 30,000 grid points, grid size  $h = 0.0625$  at the surface, and timestep  $\Delta t = 0.004$ . From top left to bottom right (for each approach):  $t = 0.0, 0.004, 0.008, 0.02, 0.096, 0.12, 0.14$ .

and on implicitly defined surfaces, where the equation reads as

$$(6.1) \quad u_t = |(I - \nu \otimes \nu) \nabla u| \left( \frac{1}{|\nabla \phi|} \nabla \cdot |\nabla \phi| \frac{(I - \nu \otimes \nu) \nabla u}{|(I - \nu \otimes \nu) \nabla u|} - 2\lambda(u - u_0) \right).$$

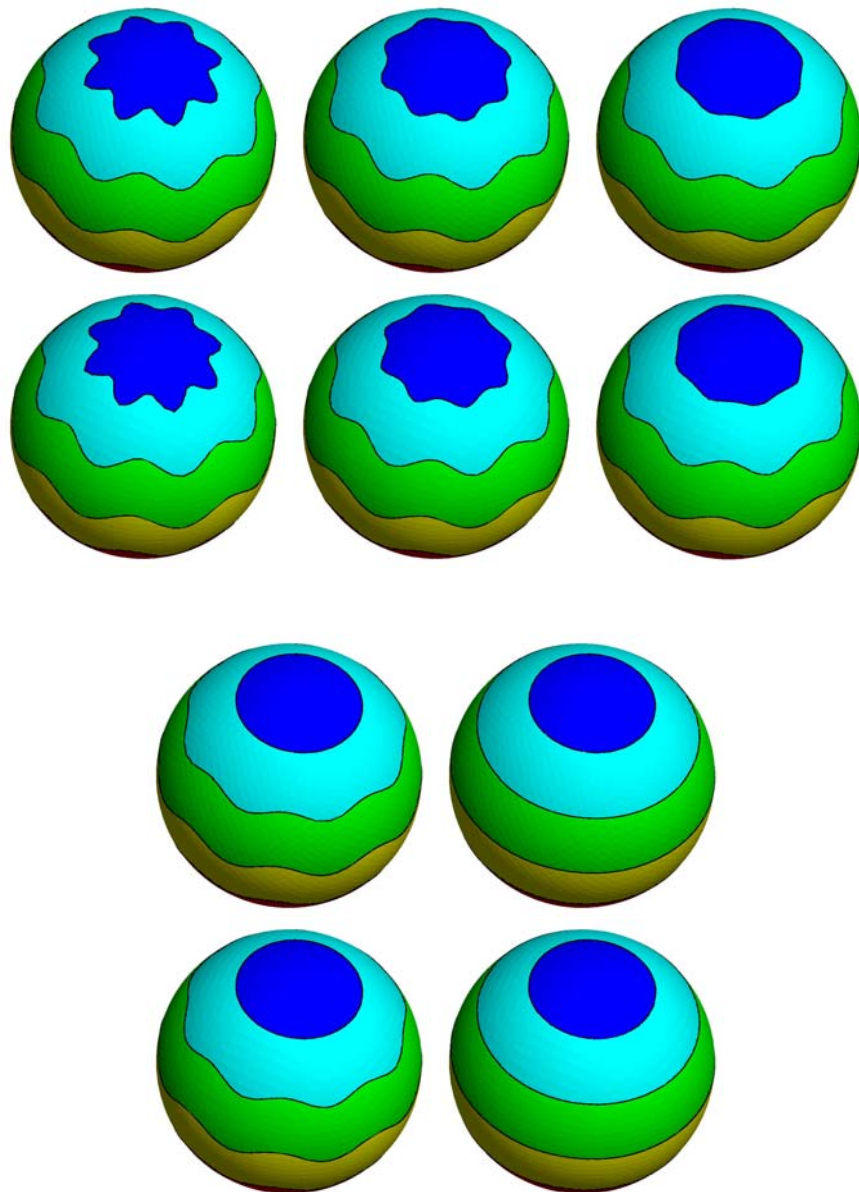


**Figure 6.** Geodesic surface diffusion with parameterization of the surface (first and third rows) and level-set representation of the surface (second and fourth rows). Parametric approach: 3,000 grid points, grid size  $h = 0.064$ , and timestep  $\Delta t = 1.0 \times 10^{-5}$ . Level-set approach:  $[0, 4] \times [0, 4] \times [0, 4]$  grid with 30,000 grid points, grid size  $h = 0.0625$  at the surface, and timestep  $\Delta t = 1.0 \times 10^{-5}$ . From top left to bottom right (for each approach):  $t = 0.0, 0.00002, 0.00004, 0.0001, 0.001$ .

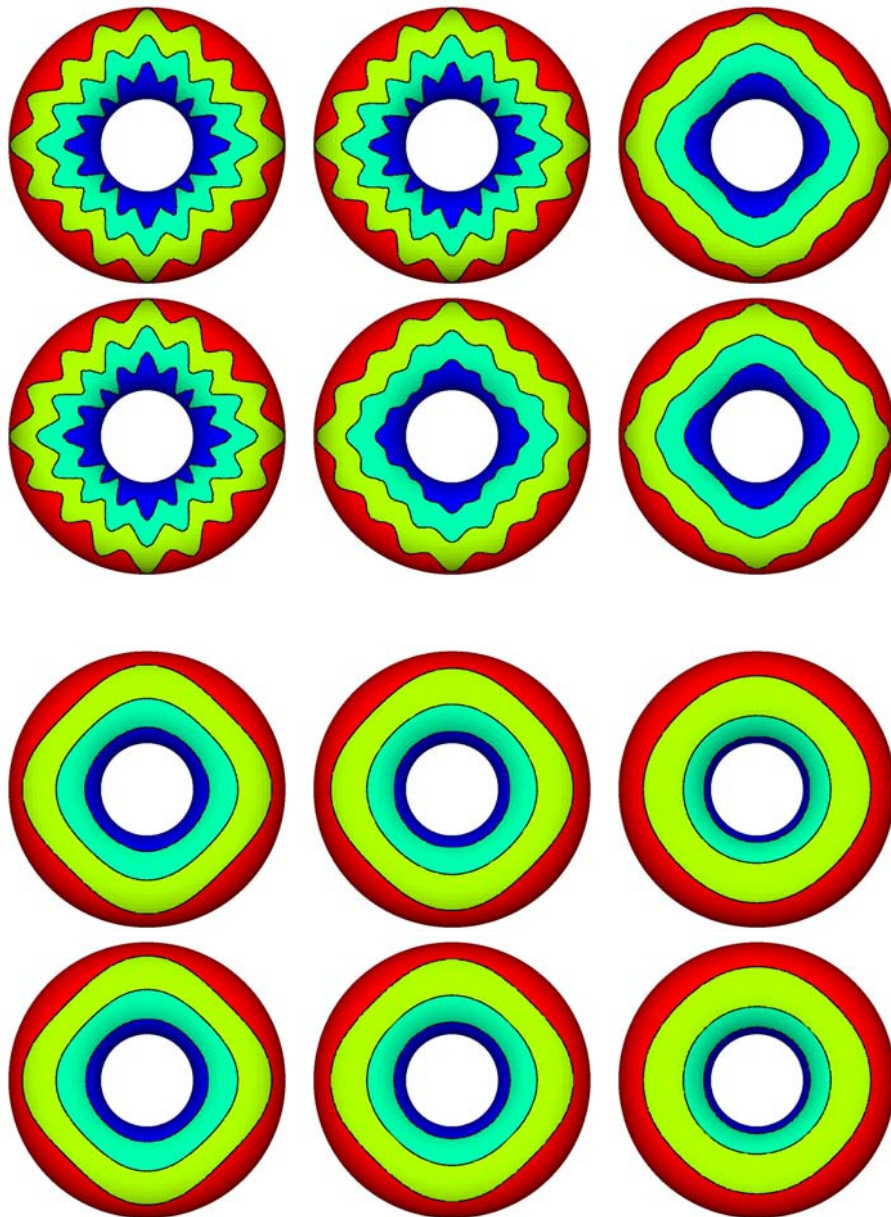


**Figure 7.** Geodesic mean curvature flow with parameterization of the surface (first and third rows) and level-set representation of the surface (second and fourth rows). Parametric approach: 8,200 grid points, grid size  $h = 0.048$ , and timestep  $\Delta t = 0.001$ . Level-set approach:  $[0, 4] \times [0, 4] \times [0, 4]$  grid with 91,000 grid points, grid size  $h = 0.005$  at the surface, and timestep  $\Delta t = 0.001$ . From top left to bottom right (for each approach):  $t = 0.0, 0.004, 0.01, 0.06, 0.1, 0.2$ .

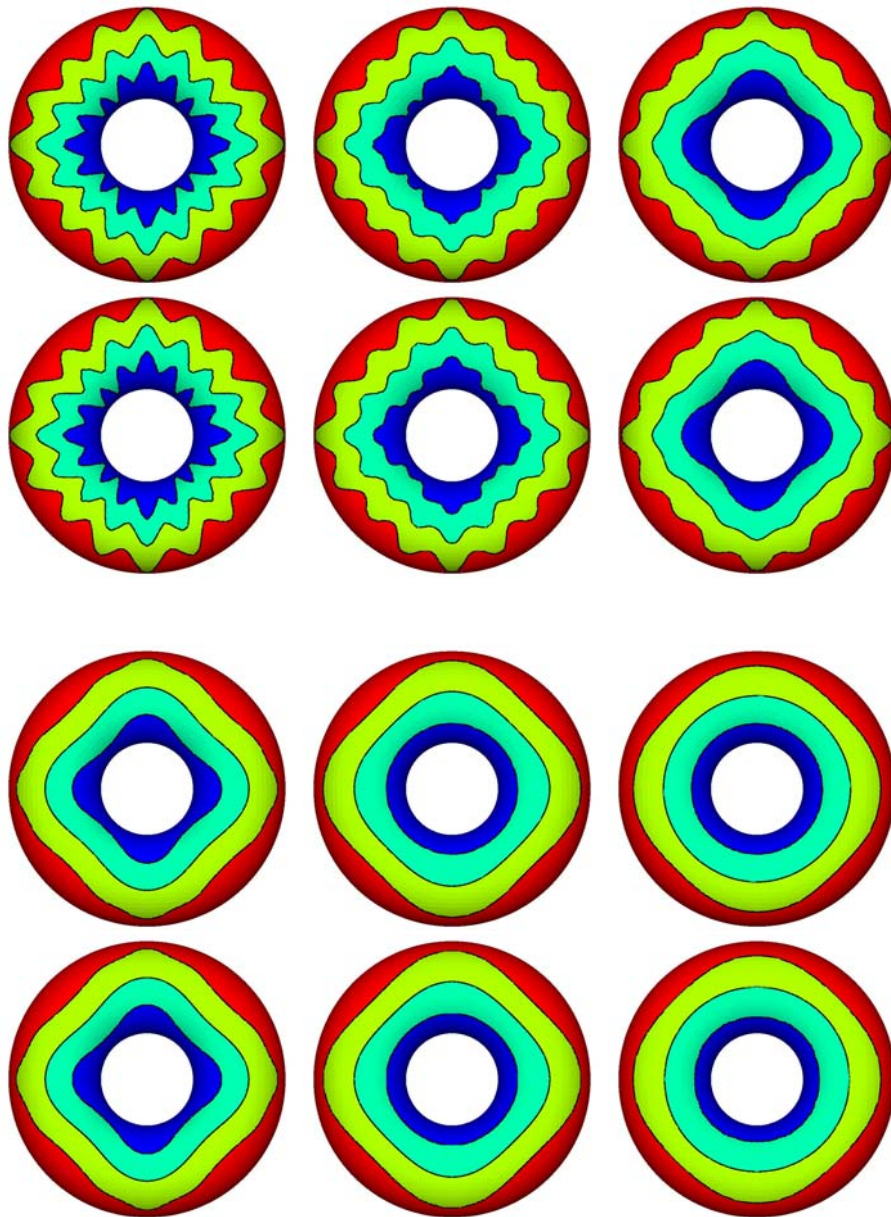


**Figure 8.** Geodesic surface diffusion with parameterization of the surface (first and third rows) and level-set representation of the surface (second and fourth rows). Parametric approach: 8,200 grid points, grid size  $h = 0.048$ , and timestep  $\Delta t = 5.0 \times 10^{-6}$ . Level-set approach:  $[0, 4] \times [0, 4] \times [0, 4]$  grid with 91,000 grid points, grid size  $h = 0.005$  at the surface, and timestep  $\Delta t = 5.0 \times 10^{-6}$ . From top left to bottom right (for each approach):  $t = 0.0, 0.00002, 0.00005, 0.0002, 0.003, 0.012$ .

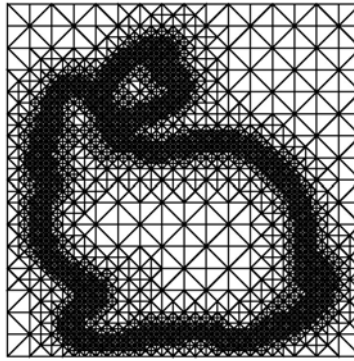


**Figure 9.** Cut-through adaptive grid used for calculations shown in Figures 10 and 11. Adaptive grid refinement at the implicit surface  $\phi = 0$ . The complete grid has 192,000 grid points.

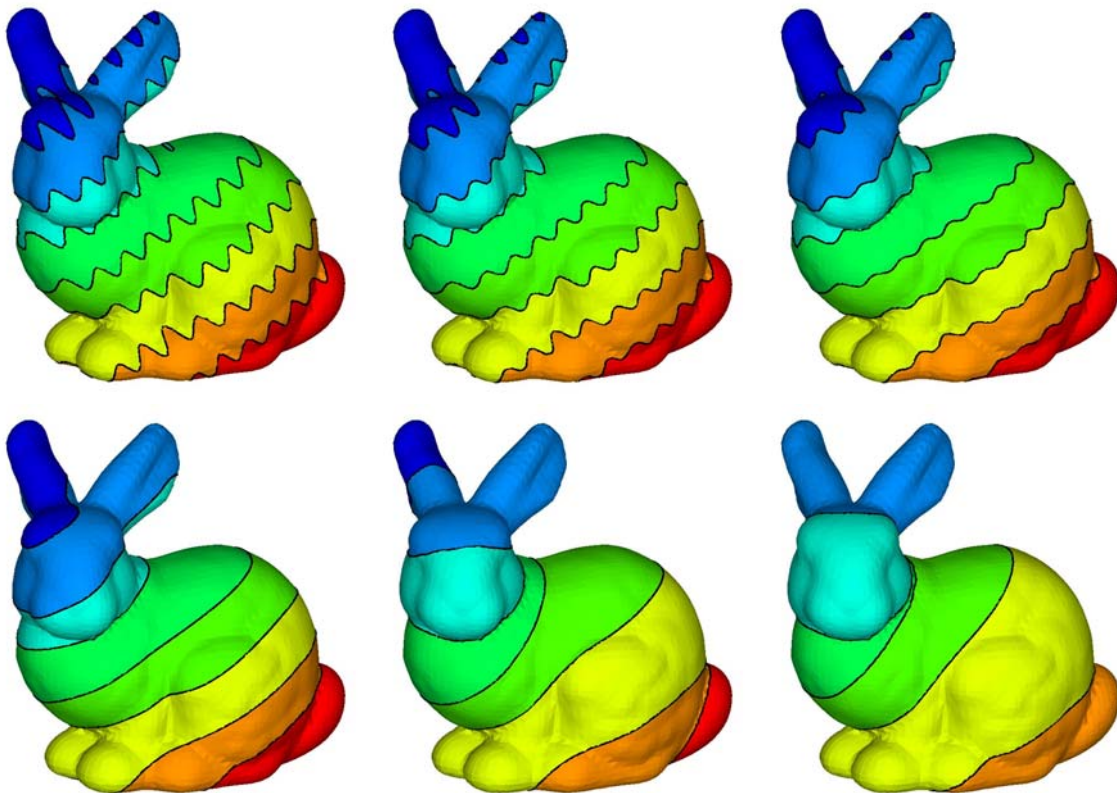


**Figure 10.** Geodesic mean curvature flow with level-set representation of the surface: evolution of different level sets.  $[0, 4] \times [0, 4] \times [0, 4]$  grid with 192,000 grid points, grid size  $h = 0.039$  at the surface, and timestep  $\Delta t = 0.001$ . From top left to bottom right:  $t = 0.0$ ,  $t = 0.002$ ,  $t = 0.005$ ,  $t = 0.04$ ,  $t = 1.0$ ,  $t = 1.8$ .

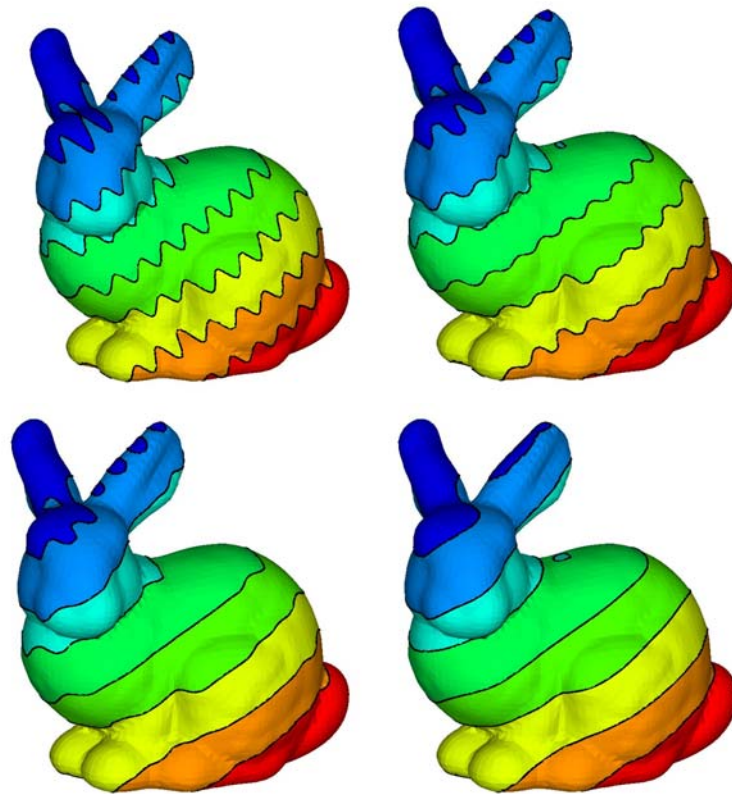


**Figure 11.** Geodesic surface diffusion with level-set representation of the surface: evolution of different level sets.  $[0, 4] \times [0, 4] \times [0, 4]$  grid with 192,000 grid points, grid size  $h = 0.039$  at the surface, and timestep  $\Delta t = 2.5 \times 10^{-6}$ . From top left to bottom right:  $t = 0.0$ ,  $t = 0.00002$ ,  $t = 0.00005$ ,  $t = 0.0003$ .

The last equation has been solved numerically with finite differences in [4]. The authors in [4] also extend the calculation of the forcing term coefficient  $\lambda$  from the situation in  $\mathbb{R}^{n+1}$  given in [29] to implicitly given surfaces. The idea is as follows: when steady state is reached, the term on the left-hand side vanishes. Multiplication with  $|\nabla\phi|(u - u_0)$  and integration by parts results in

$$\lambda = -\frac{1}{2\sigma^2} \int_{\Omega} |\nabla\phi| \frac{(I - \nu \otimes \nu)\nabla u}{|(I - \nu \otimes \nu)\nabla u|} \cdot \nabla(u - u_0) dx$$

with noise parameter  $\sigma^2 = \int_{\Omega} |\nabla\phi|(u - u_0)^2 dx$ . We now use this model to demonstrate the possibility of updating existing models in image processing to surfaces. For image denoising on implicitly defined surfaces the weak form of (6.1) is given through

$$\begin{aligned} & \int_{\Omega} \frac{u_t |\nabla\phi|}{|(I - \nu \otimes \nu)\nabla u|} \eta dx \\ &= - \int_{\Omega} |\nabla\phi| \frac{(I - \nu \otimes \nu)\nabla u}{|(I - \nu \otimes \nu)\nabla u|} \cdot \nabla\eta dx - 2\lambda \int_{\Omega} |\nabla\phi| (u - u_0) \eta dx. \end{aligned}$$

The discretization for image denoising reads as

$$\begin{aligned}
 (6.2) \quad & \int_{\Omega} \frac{u^{k+1} |\nabla \phi|_{\epsilon}}{|(I - \nu \otimes \nu) \nabla u^k|_{\epsilon}} \eta \, dx - \int_{\Omega} \frac{u^k |\nabla \phi|_{\epsilon}}{|(I - \nu \otimes \nu) \nabla u^k|_{\epsilon}} \eta \, dx \\
 & + \tau \int_{\Omega} |\nabla \phi|_{\epsilon} \frac{(I - \nu \otimes \nu) \nabla u^{k+1}}{|(I - \nu \otimes \nu) \nabla u^k|_{\epsilon}} \cdot \nabla \eta \, dx \\
 & + \tau 2\lambda^k \int_{\Omega} |\nabla \phi|_{\epsilon} u^{k+1} \eta \, dx - \tau 2\lambda^k \int_{\Omega} |\nabla \phi|_{\epsilon} u_0 \eta \, dx = 0.
 \end{aligned}$$

The forcing term coefficient  $\lambda^k$  depends on the solution  $u^k$  of the last timestep and has to be calculated in each timestep in a preprocessing step through

$$\lambda^k = -\frac{1}{2\sigma^2} \int_{\Omega} |\nabla \phi|_{\epsilon} \frac{(I - \nu \otimes \nu) \nabla u^k}{|(I - \nu \otimes \nu) \nabla u^k|_{\epsilon}} \cdot \nabla (u^k - u_0) \, dx.$$

Note that  $\sigma^2$  is a fixed noise parameter, which is an estimation of the amount of noise in the initial image. To conclude we present the linear system. With

$$\begin{aligned}
 M_1 &:= M[|\nabla \phi|_{\epsilon} |(I - \nu \otimes \nu) \nabla u^k|_{\epsilon}^{-1}], \\
 M_2 &:= M[|\nabla \phi|_{\epsilon}], \\
 L_1 &:= L[|\nabla \phi|_{\epsilon} |(I - \nu \otimes \nu) \nabla u^k|_{\epsilon}^{-1} (I - \nu \otimes \nu)], \\
 R_1 &:= \left( \int_{\Omega} |\nabla \phi|_{\epsilon} u_0 \varphi_i \, dx \right)_i,
 \end{aligned}$$

the linear system corresponding to (6.2) is

$$(M_1 + \tau L_1 + \tau 2\lambda^k M_2) \bar{u}^{k+1} = M_1 \bar{u}^k + \tau 2\lambda^k R_1.$$

Again, we solve the linear system with the Krylov subspace method BiCGStab2.

Figure 12 shows results of the approach on the bunny, and Figure 13 shows a comparison between the implicit and the parametric surface representation for image denoising on the torus.

In a similar way, other variational models established to process images in  $\mathbb{R}^2$  can be reformulated to deal with images defined on surfaces. The basic ingredients for second and fourth order problems are given in this paper. Whether an explicit or implicit representation of the surface should be used will depend on the availability of an appropriate surface mesh. The numerical results are indistinguishable; the computational costs for the implicit representation, however, are higher.

**Acknowledgments.** The authors thank Gerd Dziuk and Charlie Elliott for helpful discussions. They also acknowledge the computing power provided at ZIH at TU Dresden.



**Figure 12.** Image denoising with level-set representation of the surface. From left to right: original image, noisy image, image after 5 timesteps.  $[0, 4] \times [0, 4] \times [0, 4]$  grid with 192,000 grid points, grid size  $h = 0.039$  at the surface, and timestep  $\Delta t = 0.001$ .

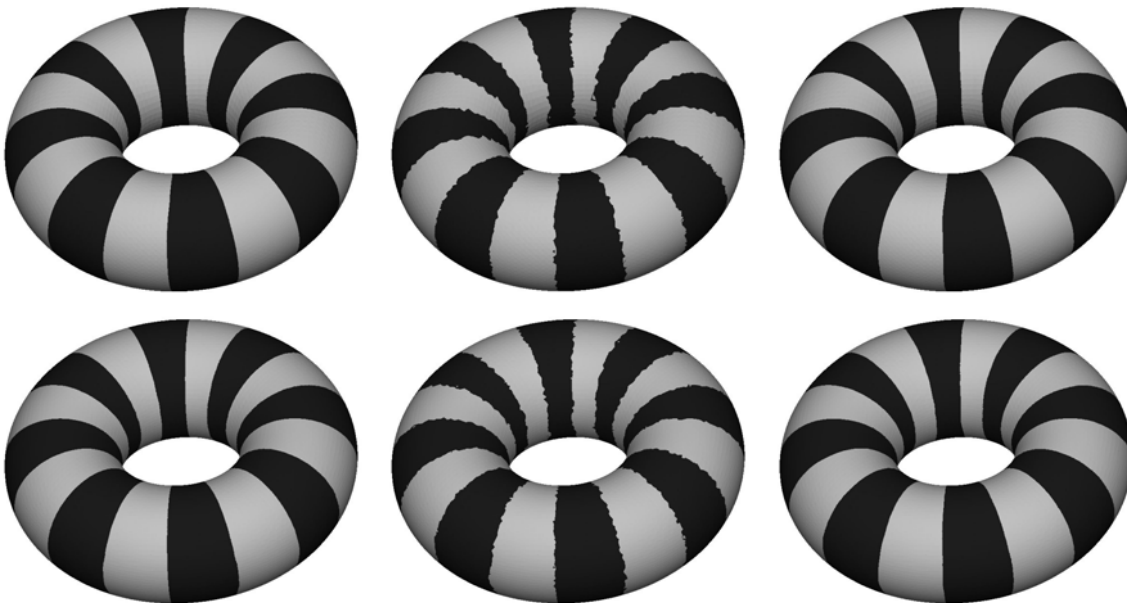


**Figure 13.** Image denoising with parameterization of the surface (top row) and level-set representation of the surface (bottom row). From left to right: original image, noisy image, image after 5 timesteps. Parametric approach: 16,500 grid points, grid size  $h = 0.034$ , and timestep  $\Delta t = 0.001$ . Level-set approach:  $[0, 4] \times [0, 4] \times [0, 4]$  grid with 193,000 grid points, grid size  $h = 0.03125$  at the surface, and timestep  $\Delta t = 0.001$ .

## REFERENCES

- [1] D. ADELSTEINSSON AND J. A. SETHIAN, *Transport and diffusion of material quantities on propagating interfaces via level set methods*, J. Comput. Phys., 185 (2003), pp. 271–288.
- [2] C. L. BAJAJ AND G. XU, *Anisotropic diffusion of surfaces and functions on surfaces*, ACM Trans. Graph., 22 (2003), pp. 4–32.
- [3] T. J. BARTH AND J. A. SETHIAN, *Numerical schemes for the Hamilton-Jacobi and level set equations on triangulated domains*, J. Comput. Phys., 145 (1998), pp. 1–40.
- [4] M. BERTALMÍO, L.-T. CHENG, S. OSHER, AND G. SAPIRO, *Variational problems and partial differential equations on implicit surfaces*, J. Comput. Phys., 174 (2001), pp. 759–780.
- [5] A. L. BERTOZZI, S. ESEDOGLU, AND A. GILLETTE, *Inpainting of binary images using the Cahn-Hilliard equation*, IEEE Trans. Image Process., 16 (2007), pp. 285–291.
- [6] T. F. CHAN AND J. SHEN, *Image Processing and Analysis: Variational, PDE, Wavelet, and Stochastic Methods*, SIAM, Philadelphia, 2005.
- [7] L.-T. CHENG, P. BURCHARD, B. MERRIMAN, AND S. OSHER, *Motion of curves constrained on surfaces using a level-set approach*, J. Comput. Phys., 175 (2002), pp. 604–644.
- [8] D. L. CHOPP AND J. A. SETHIAN, *Flow under curvature: Singularity formation, minimal surfaces, and geodesics*, Experiment. Math., 2 (1993), pp. 235–255.
- [9] D. L. CHOPP AND J. A. SETHIAN, *Motion by intrinsic Laplacian of curvature*, Interfaces Free Bound., 1 (1999), pp. 107–123.
- [10] U. CLARENZ, U. DIEWALD, AND M. RUMPF, *Anisotropic geometric diffusion in surface processing*, in IEEE Visualization, Proceedings of the Conference on Visualization '00, 2000, pp. 397–505.
- [11] U. CLARENZ, F. HAUSSER, M. RUMPF, A. VOIGT, AND U. WEIKARD, *On level set formulations for anisotropic mean curvature flow and surface diffusion*, in Multiscale Modeling in Epitaxial Growth, Internat. Ser. Numer. Math. 149, Birkhäuser, Basel, 2005, pp. 227–237.
- [12] K. DECKELNICK, G. DZIUK, AND C. M. ELLIOTT, *Computation of geometric partial differential equations and mean curvature flow*, Acta Numer., 14 (2005), pp. 139–232.
- [13] M. DESBRUN, M. MEYER, P. SCHRÖDER, AND A. H. BARR, *Implicit fairing of irregular meshes using diffusion and curvature flow*, in Proceedings of the 26th Annual Conference on Computer Graphics and Interactive Techniques (SIGGRAPH '99), ACM, New York, 1999, pp. 317–324.
- [14] G. DZIUK, *An algorithm for evolutionary surfaces*, Numer. Math., 58 (1991), pp. 603–611.
- [15] G. DZIUK AND C. M. ELLIOTT, *Finite elements on evolving surfaces*, IMA J. Numer. Anal., 27 (2007), pp. 262–292.
- [16] G. DZIUK AND C. M. ELLIOTT, *Surface finite elements for parabolic equations*, J. Comput. Math., 25 (2007), pp. 385–407.
- [17] G. DZIUK AND C. M. ELLIOTT, *Eulerian finite element method for parabolic PDEs on implicit surfaces*, Interfaces Free Bound., 10 (2008), pp. 119–138.
- [18] J. B. GREER, A. L. BERTOZZI, AND G. SAPIRO, *Fourth order partial differential equations on general geometries*, J. Comput. Phys., 216 (2006), pp. 216–246.
- [19] R. KIMMEL, *Intrinsic scale space for images on surfaces: The geodesic curvature flow*, Graph. Models Image Process., 59 (1997), pp. 365–372.
- [20] R. KIMMEL, *Numerical Geometry of Images: Theory, Algorithms, and Applications*, Springer-Verlag, New York, 2003.
- [21] J. S. LOWENGRUB, J.-J. XU, AND A. VOIGT, *Surface phase separation and flow in a simple model of multicomponent drops and vesicles*, FDMP Fluid Dyn. Mater. Process., 3 (2007), pp. 1–19.
- [22] M. LYSAKER, A. LUNDERVOLD, AND X.-C. TAI, *Noise removal using fourth-order partial differential equation with applications to medical magnetic resonance images in space and time*, IEEE Trans. Image Process., 12 (2003), pp. 1579–1590.
- [23] J. MALIK AND P. PERONA, *Scale-space and edge-detection using anisotropic diffusion*, IEEE Trans. Pattern Anal. Mach. Intell., 12 (1990), pp. 629–639.
- [24] A. MARQUINA AND S. OSHER, *Explicit algorithms for a new time dependent model based on level set motion for nonlinear deblurring and noise removal*, SIAM J. Sci. Comput., 22 (2000), pp. 387–405.
- [25] S. OSHER AND J. A. SETHIAN, *Fronts propagating with curvature-dependent speed: Algorithms based on Hamilton-Jacobi formulations*, J. Comput. Phys., 79 (1988), pp. 12–49.

- [26] S. OSHER, A. SOLÉ, AND L. VESE, *Image decomposition and restoration using total variation minimization and the  $H^{-1}$  norm*, Multiscale Model. Simul., 1 (2003), pp. 349–370.
- [27] A. RÄTZ AND A. VOIGT, *PDE's on surfaces—a diffuse interface approach*, Commun. Math. Sci., 4 (2006), pp. 575–590.
- [28] A. RÄTZ AND A. VOIGT, *A diffuse-interface approximation for surface diffusion including adatoms*, Nonlinearity, 20 (2007), pp. 177–192.
- [29] L. RUDIN, S. OSHER, AND E. FATEMI, *Nonlinear total variation based noise removal algorithms*, Phys. D, 60 (1992), pp. 259–268.
- [30] G. SAPIRO, *Geometric Partial Differential Equations and Image Analysis*, Cambridge University Press, Cambridge, UK, 2006.
- [31] P. SMEREKA, *Semi-implicit level set methods for curvature and surface diffusion motion*, J. Sci. Comput., 19 (2003), pp. 439–456.
- [32] A. SPIRA AND R. KIMMEL, *Geometric curve flows on parametric manifolds*, J. Comput. Phys., 223 (2007), pp. 235–249.
- [33] C. STÖCKER AND A. VOIGT, *A level set approach to anisotropic surface evolution with free adatoms*, SIAM J. Appl. Math., 69 (2008), pp. 64–80.
- [34] S. VEY AND A. VOIGT, *AMDiS: Adaptive multidimensional simulations*, Comput. Vis. Sci., 10 (2007), pp. 57–67.
- [35] J. WEICKERT, *Anisotropic Diffusion in Image Processing*, Teubner, Stuttgart, 1998.
- [36] J.-J. XU AND H.-K. ZHAO, *An Eulerian formulation for solving partial differential equations along a moving interface*, J. Sci. Comput., 19 (2003), pp. 573–594.